

Effect of Disulfide Bridge on the Binding of SARS-CoV-2 Fusion Peptide to Cell Membrane: a Coarse-Grained Study

Hujun Shen,^{1*} Zhenhua Wu²

1. *Guizhou Provincial Key Laboratory of Computational Nano-Material Science, Guizhou Education University, Guiyang 550018, China.*

2. *Department of Big Data and Artificial Intelligence, Guizhou Vocational Technology College of Electronics & Information, Kaili, 556000, China.*

Supporting Information

* Corresponding author. E-mail address: hujun.shen@hotmail.com (Hujun Shen)

Figure S1. CAVS CG representation for water. Four atomistic water molecules are grouped into a collective unit that contains two positively charged (CGP) particles, one van der Waals (vdW) interaction center (CGM) and one virtual site (CGN) carrying a negative charge ($-2q$). The bonds formed between CGM and CGPs are constrained at a distance of d and a harmonic potential is applied to the angle CGP-CGM-CGP.

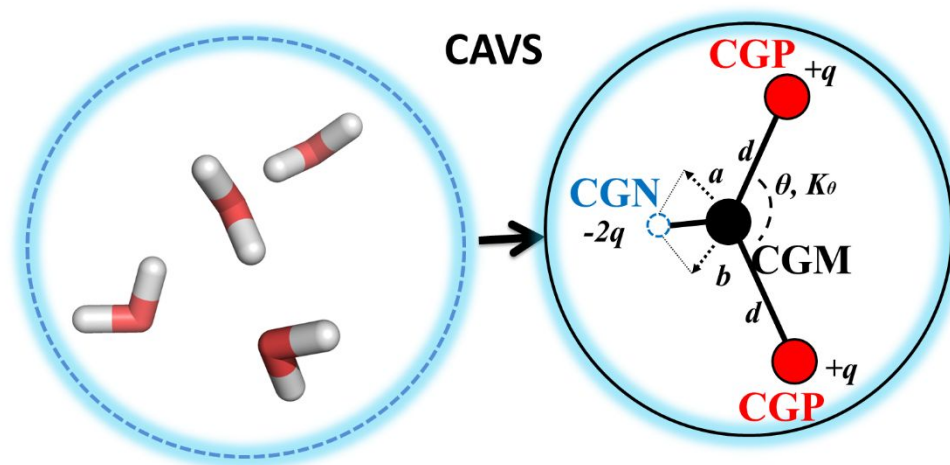
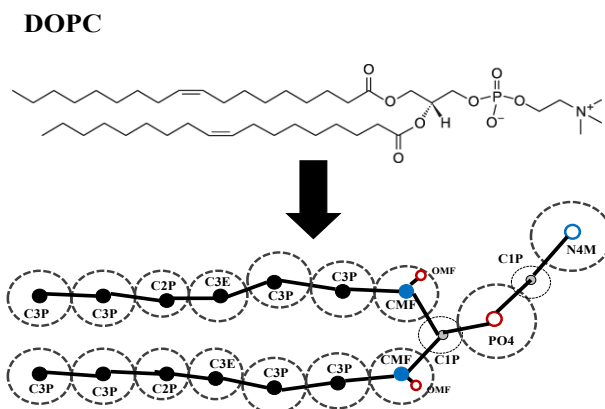
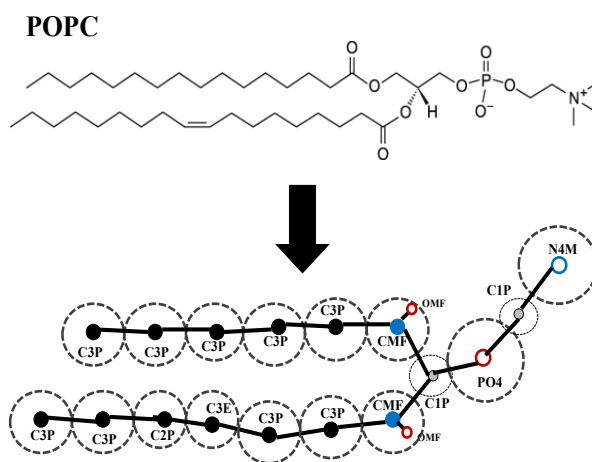


Figure S2. CAVS CG mapping for the (A) DOPC, (B) POPC and (C) POPE lipid models, the type name for each site is given in black color while the name for each CG unit is given in blue color accordingly. The neutral, non-interacting, positively charged, and negatively charged sites are denoted by the black filled, black open, red open or filled and blue filled circles respectively.

(A)



(B)



(C)

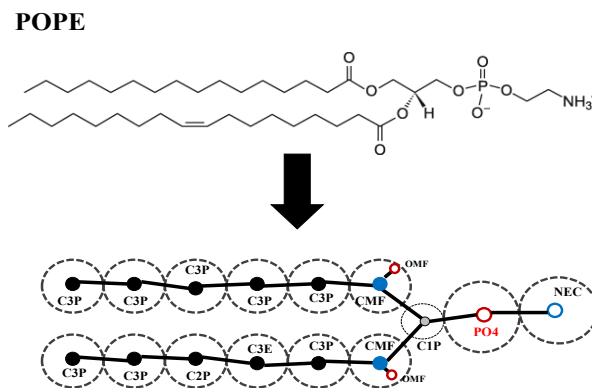


Figure S3. Corresponding all-atom structures of reduced CG beads in the CAVS CG model.

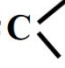
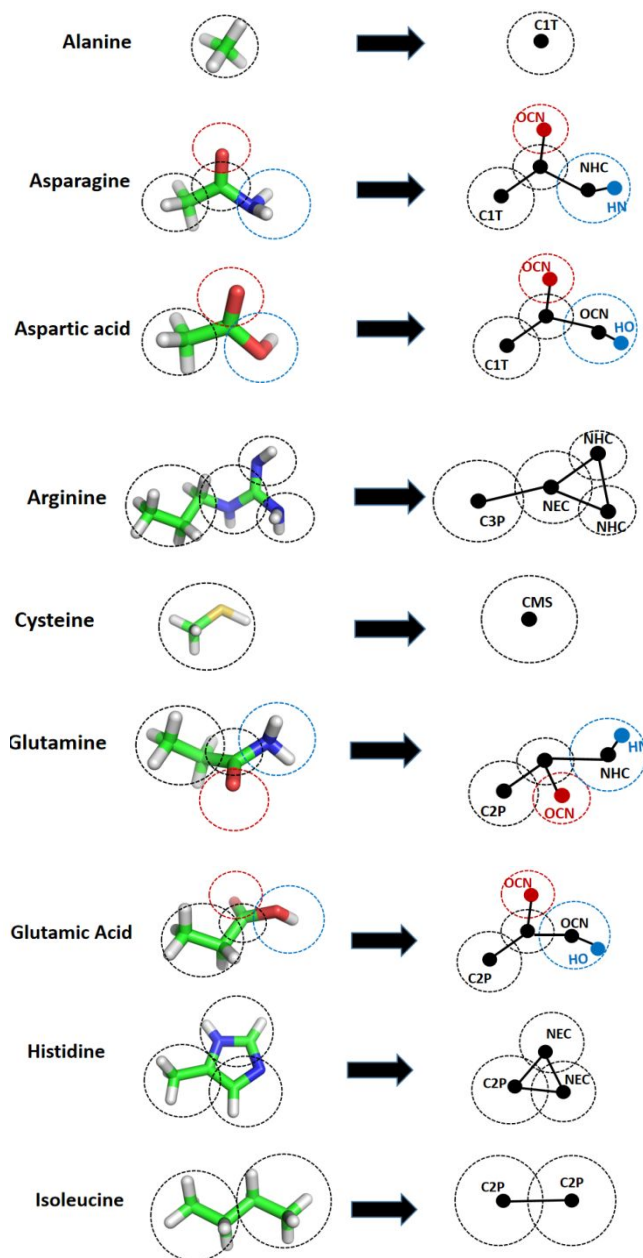
all-atom structure		CG bead
—CH_3	\Rightarrow	C1T
=O	\Rightarrow	OCN
=C 	\Rightarrow	CON
—NH—	\Rightarrow	NHC
$\text{—NHCH}_2\text{—}$	\Rightarrow	NEC
$\text{—}\overset{\text{I}}{\text{C}}\text{—}$	\Rightarrow	CAN
$\text{—CH}_2\text{CH}_2\text{—}$	\Rightarrow	C2P
$\text{—CH}_2\text{CH}_2\text{CH}_2\text{—}$	\Rightarrow	C3P
—CH=CH—	\Rightarrow	C2E
$\text{—CH=CHCH}_2\text{—}$	\Rightarrow	C3E
$\text{—CH}_2\text{SH}$	\Rightarrow	CMS
$\text{—CH}_2\text{OH}$	\Rightarrow	CMO
$\text{—CH}_2\text{CH}_2\text{OH}$	\Rightarrow	CEO

Figure S4. CAVS CG mapping for the side chain analogs of 19 amino acids.



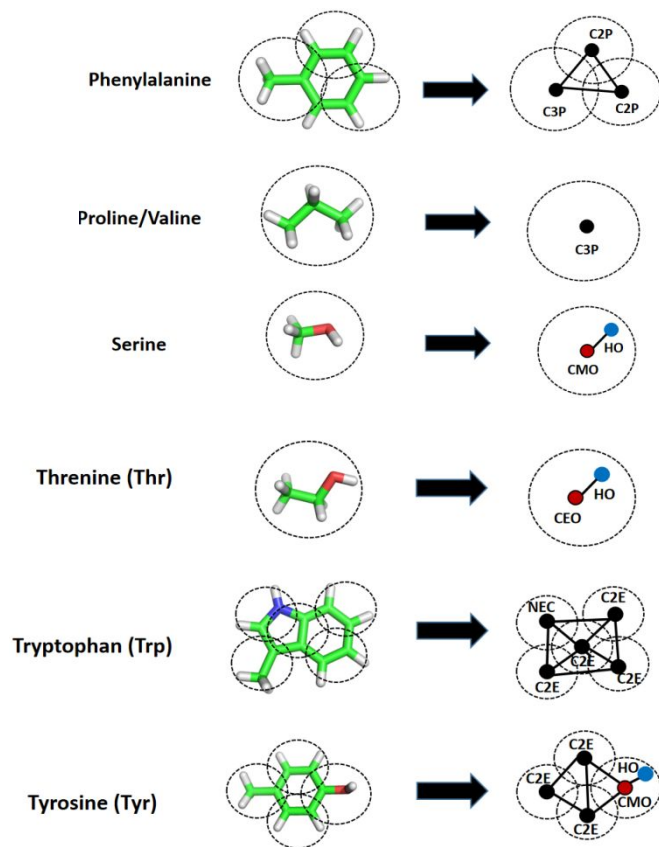
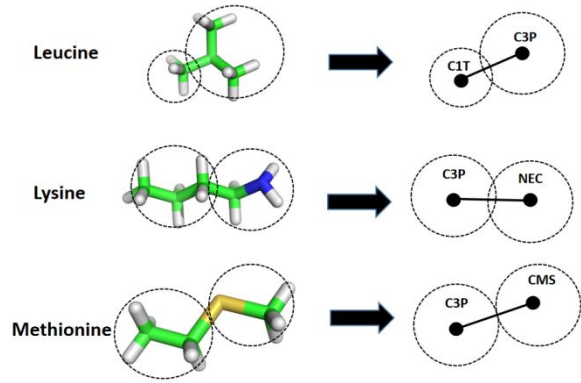


Figure S5. Definition of the tilt angle between the C17-C3 vector of cholesterol molecule and the bilayer normal (z-axis).

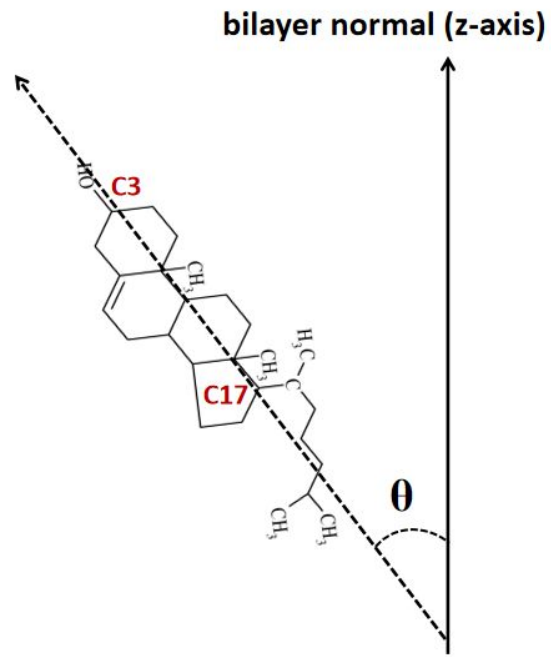
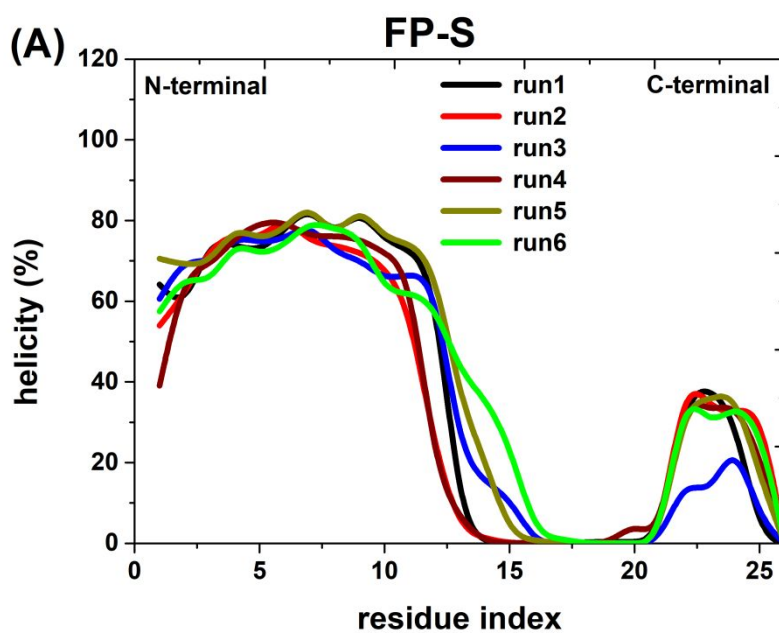


Figure S6. Helicity per residue for the (A) FP-S and (B) FP-L, obtained from six independent CAVS CG simulations of the FPs (FP-S and FP-L) with the POPC/cholesterol bilayer.



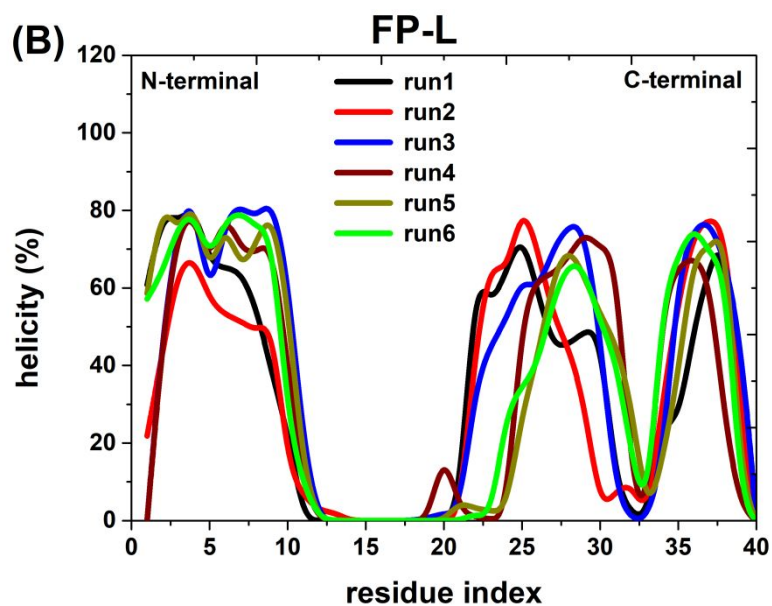
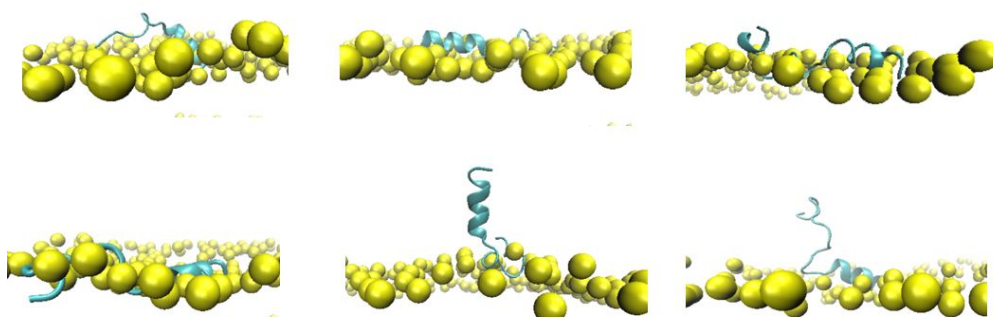


Figure S7. Six membrane-binding models of (A) SARS-CoV-2 FP-S and (B) SARS-CoV-2 FP-L were used for the constant-velocity pulling simulations. The FP-S (cyan) and FP-L (blue) are given in the cartoon representation and the phosphate groups in the space-filling representation.

(A) Membrane-binding models of SARS-CoV-2 FP-S



(B) Membrane-binding models of SARS-CoV-2 FP-L

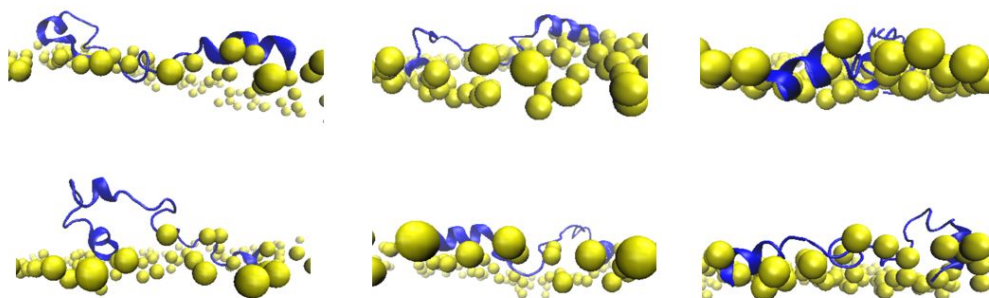


Figure S8. Helicity per residue for the FP-L-SS (black) and FP-L-noSS (red), calculated from the 1.0- μ s CAVS CG simulations of the FP-L with disulfide bond (FP-L-SS) and the FP-L with broken disulfide bond (FP-L-noSS) in aqueous solution (0.15 M NaCl).

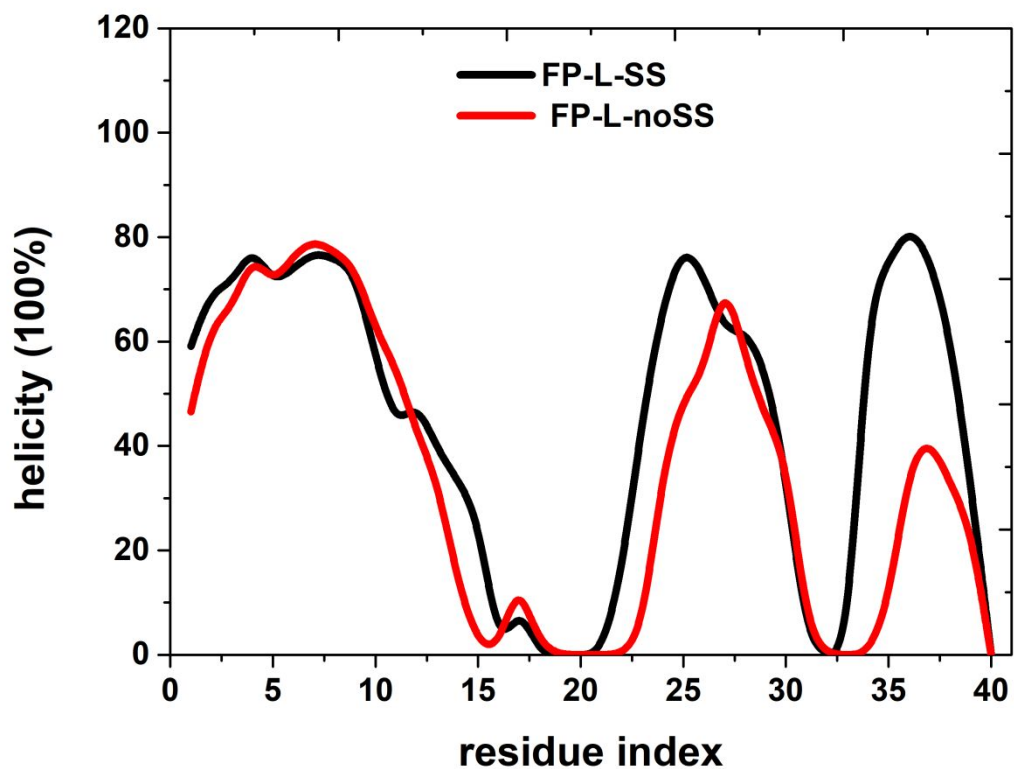


Table S1 Constrained distances between two consecutive CG beads in the CAVS protein model.

CG bead (<i>i</i>)	CG bead (<i>j</i>)	Distance (nm)
CIT	CON	0.15
CON	OCN	0.12
CON	NHC	0.13
NHC	CIT	0.15

CAN	C1T	0.15
CAN	C3P	0.25
CAN	C2P	0.20
CAN	C2E	0.20
CAN	CMO	0.20
CAN	CEO	0.25
CAN	CMS	0.20
C2E	NEC	0.20
NEC	NEC	0.20
C2P	C2P	0.20
C1T	C3P	0.20
C3P	NEC	0.26
C2P	CMS	0.20
C3E	C2E	0.30
C2E	C2E	0.25
C3E	C3E	0.30
C3E	NEC	0.35
C2E	CEO	0.25
C3E	CEO	0.30

Table S2. The parameters in the angle bending potential of the CAVS CG model

CG bead (<i>i</i>)	CG bead (<i>j</i>)	CG bead (<i>k</i>)	Equilibrium Angle (degree)	Force constant (kJ/mol)
C1T	CON	NHC	120	600
C1T	CON	OCN	120	600
OCN	CON	NHC	120	600
CON	NHC	C1T	120	600

NHC	CAN	C1T	110	600
NHC	CAN	C2P	110	600
NHC	CAN	C2E	110	600
NHC	CAN	C3P	110	600
HNC	CAN	CMS	110	600
NHC	CAN	CMO	110	600
NHC	CAN	CEO	110	600
CAN	C3P	NEC	180	300
CAN	C2E	NEC	120	300
CAN	C2P	C2P	110	300
CAN	C1T	C2P	110	300
CAN	C3P	NEC	180	300
CAN	C2P	CMS	180	300
CAN	C3E	C2E	120	600

Table S3. The parameters in the dihedral angle potential of the CAVS CG model.

CG bead (<i>i</i>)	CG bead (<i>j</i>)	CG bead (<i>k</i>)	CG bead (<i>l</i>)	Equilibrium value (degree)	Force constant (kJ/mol)	multitude
C1T	CON	NHC	C1T	180	20	2

OCN	CON	NHC	C1T	180	20	2
CAN	NHC	C1T	CON	-30	16	
CON	C1T	OCN	NHC	0	100	
CON	CAN	OCN	NHC	0	100	
CON	NHC	CAN	CON	0	2.5	3
CON	NHC	CAN	CON	0	1.5	1
CON	NHC	CAN	CON	180	3.0	2
CON	NHC	CAN	CON	180	6.0	1
NHC	CAN	CON	NHC	0	1.0	3
NHC	CAN	CON	NHC	0	4.1	1
NHC	CAN	CON	NHC	180	2.1	2
NHC	CAN	CON	NHC	180	4.0	1

Table S4 Pair-wise vdW parameters for various CG types in the CAVS protein model.

CG Type (<i>i</i>)	CG Type (<i>j</i>)	Range parameter σ (nm)	Well depth ϵ (kJ/mol)
C1T	C1T	0.39	1.00
CON	CON	0.34	0.36
OCN	OCN	0.30	0.9

NHC	NHC	0.32	0.7
CGW	CGW	0.485	4.5
PO4	PO4	0.50	5.0
N4M	N4M	0.52	4.5
CMF	CMF	0.45	4.8
C1T	C1T	0.39	1.0
C2P	C2P	0.44	1.5
C3P	C3P	0.47	2.5
C2E	C2E	0.40	1.5
C3E	C3E	0.47	2.2
NEC	NEC	0.43	3.3
CMS	CMS	0.44	2.0
CEO	CEO	0.46	5.5
CMO	CMO	0.40	5.0
NA	NA	0.33	0.01
CL	CL	0.44	0.50
CGW	C1T	0.42	1.2
CGW	CON	0.42	1.2
CGW	OCN	0.40	5.0
CGW	NHC	0.42	5.0
CGW	C3P	0.47	2.2
CGW	C2P	0.45	1.5
CGW	C3E	0.47	2.3
CGW	C2E	0.46	2.1
CGW	PO4	0.48	7.5
CGW	N4M	0.48	5.5
CGW	CMF	0.48	4.2
CGW	CMO	0.45	4.9
CGW	CEO	0.46	5.1
CGW	CMS	0.43	3.0
CEO	CEO	0.46	5.5
CEO	C1T	0.42	1.2
CEO	CON	0.41	1.0
CEO	OCN	0.40	4.0
CEO	NHC	0.41	5.0
C3P	C3P	0.47	2.5
C3P	C1T	0.44	1.5
C3P	CON	0.42	1.0
C3P	OCN	0.41	1.0
C3P	NHC	0.43	1.5
C3P	NEC	0.46	2.3
C1T	CON	0.38	0.4
C1T	OCN	0.36	0.4

C1T	NHC	0.38	0.6
C1T	NEC	0.42	0.9
NEC	CON	0.42	0.9
NEC	OCN	0.40	3.0
NEC	NHC	0.42	3.0
C1T	PO4	0.42	1.0
CON	PO4	0.42	1.0
OCN	PO4	0.40	4.5
NHC	PO4	0.42	4.5
NEC	PO4	0.46	4.7
C1T	N4M	0.42	1.5
CON	N4M	0.42	1.5
OCN	N4M	0.40	3.5
NHC	N4M	0.42	3.5
NEC	N4M	0.46	4.7
C1T	CMF	0.42	1.2
CON	CMF	0.42	1.0
OCN	CMF	0.40	3.5
NHC	CMF	0.42	3.5
NEC	CMF	0.46	4.5

Table S5. The partial charges used for the electrostatic interaction sites in the CAVS CG particles

CG particle (Amino acid)	Electrostatic interaction sites	Partial charge
OCN	OCN	-0.35

NHC	HN	0.35
NHC (Arg)	NHC	0.50
NEC (Lys)	NEC	1.0
CEO (Thr)	CMO	0.35
CEO (Thr)	OH	-0.35
CEO (Thr)	CEO	0.35
CEO (Thr)	OH	-0.35
CEO (Tyr)	CEO	0.24
CEO (Tyr)	OH	-0.24